JOINT ROUTING AND SCHEDULING FOR ELECTRIC VEHICLES IN SMART GRIDS WITH V2G

Alicia Triviño-Cabrera*, José A. Aguado, Sebastián de la Torre

Dpto. Ingeniería Eléctrica, Escuela de Ingenierías Industriales

C/ Doctor Ortiz Ramos s/n, 29071, 29071 Málaga (Spain)

{atc, jaguado, storre}@uma.es

Abstract

Modern distribution systems with high penetration of Electric Vehicles (EVs) are the focus of increasing attention. EVs charging strategies impact on power networks operation and they can even affect driving patterns when considering Vehicle-to-Grid (V2G) market-driven scenarios. This paper proposes a joint EV routing and charging/discharging scheduling strategy to operate an EV fleet. Particularly, we propose a mathematical framework based on a mixed-integer linear programming problem with the goal of maximizing the revenue of EV users. This approach is illustrated and tested using the IEEE 37-node test feeder. The results show that slight changes in driving patterns can provide benefits to EV users and improve the network operation. The correct design of the price dynamics is concluded to be key for promoting V2G participation.

Keywords:

Routing, scheduling, bidirectional, V2G, electric vehicle, charge, discharge.

NOMENCLATURE

The mathematical symbols used throughout this paper are presented and defined below.

A. Constants

N_n Number of all the nodes in the electrical network

N_{EV}	Number of all the electrical vehicles considered in the area covered by the electrical network
NC	Maximum number of chargers installed in every node.
PC_{max}	Maximum power that an electric vehicle is allowed to charge.
PI_{max}	Maximum power that an electrical vehicle is allowed to inject into the grid
PM_{max}	Maximum power consumed by the electrical vehicle when it is moving
η_{in}	Efficiency of the injecting process with energy transfer from the electric vehicle to the grid
η_{ch}	Efficiency of the charge process with energy transfer from the grid to the electric vehicle
SOC_{max}	Maximum allowable state of charge of the vehicles
SOC_{min}	Minimum allowable state of charge of the vehicles
LB	Internal losses of the battery, which occur when the vehicle is stationary and is not connected to the grid.
DoD_{max}	Maximum depth of discharge in the battery of an EV
NC_{max}	Maximum number of charge/discharge cycles that a battery in an EV can resist during its lifetime
$DistN_{n\_o,n\_d}$	Distance from node *n_o* to node *n_d, in kilometers.*
$PBcons$	Power consumed from the battery of a vehicle while moving one unit of distance
$Pcar_{bat,h}$	Power consumed from the battery of vehicle *bat* during interval *h* due to its movement
$Rdown_{gen}$	Ramping-down for the shut-down of generator type *gen*

Rup_{gen} Ramping-up for the start-up of generator type *gen*

$p\_o_{h,node}$ Price offered by the grid to buy energy at *node* during interval *h*

$p\_d_{h,node}$ Price set for the sale of energy from the EVs to the grid at *node* during interval *h*

B. Variables used to model the EV

$c_{bat,h,node}$ Binary variable that is equal to 1 if vehicle *bat* is being charged when it is connected to *node* at time *h*

$i_{bat,h,node}$ Binary variable that is equal to 1 if vehicle *bat* is injecting energy to the grid when it is connected to *node* at time *h*

$o_{bat,h}$ Binary variable that is equal to 1 if vehicle *bat* is not connected to the grid at time *h* and is stationary

$m_{bat,h}$ Binary variable that is equal to 1 if vehicle *bat* is moving at time *h*

$x_{bat,h}$ Binary variable that is equal to 1 if vehicle *bat* changes its behavior (from charging or discharging to other) at the transition from time *h* to time *h+1*

$w_{bat,h}$ Binary variable that is equal to 1 if vehicle *bat* is being charged or disconnected at time *h*. It is equal to 0 if the vehicle *bat* is injecting power to the grid at time *h*

$e_{bat,h,node}$ Binary variable that is equal to 1 if vehicle *bat* is connected to *node* at time *h*

d_{bat,h,n_o,n_d} Binary variable that is equal to 1 if vehicle *bat* is moving from node *n_o* to n_d at time *h*

$a_{bat,h,node}$ Binary variable that links the position of the vehicle *bat* (*node*) and its state of moving, charging, injecting and being disconnected at time *h*

$Pch_{bat,h,node}$ Energy charged by vehicle *bat* during time *h* when it is connected to *node*

$Pin_{bat,h,node}$ Energy injected from vehicle *bat* to the grid during time *h* when it is connected to *node*

$Pmov_{bat,h}$ Energy consumption in vehicle *bat* during time *h* when it is moving

$EVE_{bat,h,node}$ Energy delivered by the grid to vehicle *bat* at *node* during time *h*

$SOC_{bat,h}$ State of charge of vehicle *bat* at time *h*

$MaxFlow_{ni,nj}$ Maximum power flow allowed in the line connecting node *ni* to node *nj*

C. Variables used to model the electrical network

$P_{gen,node,h}$ Maximum energy delivered by the generators type *gen,* which are connected to *node,* during interval *h*

$flow_{node,h}$ Complex power at *node* at interval *h*

$SL_{node\_i,node\_j}$ Susceptance of the line connecting *node_i* to *node_j*

$\emptyset_{node,h}$ Angle voltage at *node* at interval *h*.

$Demand_{node,h}$ Complex power absorbed by the demand at *node* at interval *h*

$benefit_{day}$ Economic benefit obtained by the fleet of EVs during a day

$benefit_h$ Economic benefit obtained by the fleet of EVs during interval *h*

D. Sets

Ω_n Set of all the nodes in the electrical network.

Ω_{EV} Set of all the electrical vehicles in the area covered by the electrical network.

1. Introduction

In the mid- and long-term, it is expected that the increased number of electric vehicles will have a significant impact on the electrical network [1]. On the one hand, while charging, they will represent a considerable fraction of the total demand, which will potentially affect the network's stability and efficiency. Indeed , the uncontrolled charging of a massive number of electric vehicles could cause major power losses, voltage deviations and distribution substations overload [2]. In a unidirectional V2G (Vehicle-to-Grid) scenario [3], it is possible to control the charge, assuming that the vehicles act as deferrable loads, that is, the vehicles can be charged at specific and recommended periods. According to the demand and the generation curves, it is preferable to stimulate the charge process in those periods with a high generation and a low demand, while avoiding the periods with significant demand [4].

On the other hand, in a bidirectional V2G (Vehicle-to-Grid) context, a smart grid will also enable a bidirectional energy transfer between the vehicles and the grid [3]. If correctly managed, this bidirectional exchange is particularly suitable for coping with demand peaks or for performing ancillary services (e.g. fast frequency control) [5]. Under these circumstances, electric vehicles could behave as temporary and mobile generators/loads with a fast response time. Despite this potential benefit, the energy delivery from the vehicle batteries needs to be performed only when required by the grid. Otherwise, the energy exchange could be detrimental to the electrical and security status of the network.

Thus, when and where the electric vehicles are charged and discharged is a process that needs to be controlled through incentives or price regulations. Agents (e.g. vehicle aggregators), in coordination with grid operators, are responsible for providing recommendations on the charge/discharge process for the vehicles that they control. The recommendations are generated by means of a mathematical optimization model that considers the charging stations, the grid status and/or the users' satisfaction. The simplest solutions opt for only setting the instants at which the charge occurs. This mathematical problem is known as scheduling. The objectives of the proposed scheduling algorithms are diverse. They may aim at minimizing carbon dioxide emissions [6], [7], [8], [9], improving the integration of renewable energy sources [10], providing a better network performance [11], [12] or increasing user satisfaction (e.g. reducing driver range anxiety).

Another aspect that facilitates the integration of EVs into the grid is routing. By this approach, the vehicles could modify their conventional itinerary (classically built following the shortest path strategy) or their driving patterns in order to achieve some specific goals. The Vehicle Routing Problem (VRP) is a classic mathematical problem that tries to determine the route that a vehicle should take from its origin to its destination with a specific goal. When defining these journeys, we could set diverse objectives such as using the shortest routes, minimizing the travel time (including delays produced by traffic regulations and congestions), giving priority to the delivery of emergency goods, minimizing fuel consumption, reducing carbon emissions, satisfying some resource constraints or increasing users' satisfaction (e.g. by recommending areas with a high number of available parking spaces) [13].

Important benefits are expected when routing and scheduling techniques are both applied to generate a driver's recommendations. An EV willing to join this initiative may decide to deviate from its conventional route and driving behavior in order to charge/discharge its battery in a node that is not the final destination or is not even on the itinerary of the expected shortest journey. Routing and scheduling for electric vehicles are both addressed in previous research papers. In [14], the authors propose the application of both problems sequentially. In the first phase, they implement a modified Floyd algorithm to find the shortest route to the destination, where the vehicle is supposed to be recharged. As a novelty, it tries to keep within the charge area without exceeding a set level of traffic congestion, so that the agents may recommend closer areas to park if the vehicle is in danger of exceeding the maximum congestion level. In the second phase, the algorithm determines when the charge is going to take place. For this operation, charge costs are minimized. A similar sequential approach can be found in [15].

Alternatively, both previous mathematical problems can be formulated and solved jointly so that they help to determine the route that a vehicle should take and when its energy transfer should take place. With regard to the latter, there are algorithms for unidirectional (vehicles are not able to discharge their battery when connected to the

grid) and bidirectional V2G (vehicles may opt for activating a discharge process when connected to the network) [3].

In a unidirectional charge context, the most relevant proposals are as follows. In the context of a fleet of electric vehicles used collectively to pick up and deliver passengers, the study in [16] proposes an algorithm that minimizes travel time, route distance and charging costs to determine both the route and the charge scheduling. For the charge, the authors set mid-tour charges in order to reduce the drivers' range anxiety. An algorithm combining routing and unidirectional scheduling is also presented in [17]. This research simultaneously minimizes travel time and cost of charging the electric vehicle. For travel time, the model includes the time spent in a queue while waiting for a charger to become available. A crowd-sensing algorithm is incorporated into the system so that some information about the activity of the charger stations can be used for the routing and scheduling recommendations. The impact of the charge process on the batteries is incorporated in [18]. Particularly, they define a genetic algorithm to determine how to route and schedule the charge of a group of vehicles in order to minimize the costs of the charges and the degradation of the batteries. Fast charging is only possible along the vehicles' itinerary as in [19].

On the other hand, the joint proposal of routing and bidirectional scheduling is presented in [20]. In a similar way to [18], they restrict the chargers to the vehicle's route in order to be fast. This is the only kind of charge that is assumed to degrade the batteries, that is, to reduce battery lifetime. In fact, the authors do not discuss how the batteries' lifetime is reduced because the charge occurs while the vehicle is in the depot. In this paper, the definition of the vehicle route is based on a complex goal that aims to minimize the costs of the chargers, reducing battery degradation due to fast charges and maximizing the profits obtained by the drivers in the discharge process. The impact of the charge/discharge procedures on the grid is not analyzed. The work in [21] addresses the definition of a joint routing and bidirectional scheduling. However, important issues such as the impact on the electrical network and battery degradation are not considered.

As a novelty, in this paper we propose a joint routing and scheduling algorithm for bidirectional energy transfer that finds the optimal solution while taking into account (i) the impact of the transfer on the electrical network and (ii) a realistic degradation of the batteries due to the charge/discharge processes. In order to determine the suitability of the energy exchange parameters (electrical node to which the vehicle must be connected, amount of energy and scheduling); our proposed agent in conjunction with the electrical network aims to maximize the benefits for the driver. Thus, routing and bidirectional scheduling are solved in the same mathematical problem. Through an extensive evaluation, we demonstrate that the joint resolution of routing and scheduling leads to a better performance (in terms of user profits) than the sequential application of a routing and a scheduling problem. By combining both, the results show that some vehicles could alter their driving and charging patterns in order to obtain some profit, while the network does not suffer excessive power losses.

The main contributions of the paper are:

- It proposes to extend the classical vehicle agents in order to incorporate the routing and scheduling problems simultaneously in a bidirectional context (charge and discharge processes are considered). Thus, they recommend the time when the energy exchange between the vehicles and the grid should take place and the most convenient nodes at which to carry out this procedure, considering the final destination of the vehicle. For these recommendations, the analysis includes the origin, destination and even some intermediate nodes that an EV should include in its journey.
- Previous studies [18],[20] employ heuristic and artificial intelligence-based mechanisms to derive approximate solutions. However, our proposed algorithm is based on an optimization problem that finds the exact solution. The formulation has been carefully stated in order to reduce the number of variables needed. Consequently, computer time and resources used to solve the problem are reduced.
- The proposed approach measures the impact that the connection of the vehicles has on the grid (power losses). This effect is taken into account in [18] and in [20].
- The proposed formulation also considers the battery lifetime aspect of the problem in a realistic way. This issue has also been addressed in [18] and in [20]. However, both studies only set fast charges along the vehicle's route and assume that only this kind of charge causes battery degradation. In particular, [18] defines a fixed additional cost for each charge process. Alternatively, [20] models this cost as a function of the battery State-Of-Health. In contrast to these previous works, we take into account this degradation for all types of charge/discharge processes (even that occurring due to vehicle movement and due to vehicle charge in its base). We also model the dependence between the degradation suffered by the battery, the depth of discharge and the number of charge/discharge cycles.

The algorithm follows an approach in which each EV receives recommendations for its own route, the charging/discharging intervals and its expected revenues.

The remainder of the paper is organized as follows. Section 2 presents the mathematical model used for the characterization of the electric vehicles as mobile deferrable loads. Section 3 outlines the approach to jointly address routing and scheduling in bidirectional V2G scenarios. Section 4 explains the simulations carried out in this work and analyzes the results. Finally, Section 5 draws the main conclusions and establishes some future research guidelines.

2. Electrical and spatial model of the electric vehicle

In our problem, EVs are modeled as mobile batteries. The model includes two sets of equations to summarize (i) the EV electrical aspects and (ii) the spatial conditions

derived from their movements. Both characterizations are presented in the following subsections:

- **Electrical model**

Taking into account the electrical interaction with the grid, the EV may be receiving energy from it, injecting energy to it, or not exchanging any energy (static or moving). These four states are labeled as follows:

- Charging. The vehicle is static and its battery is being charged through the electrical network.
- Injecting. The vehicle is static and providing energy to the grid from its own battery.
- Disconnected. The vehicle is static but there is no interaction with the grid.
- Moving. The vehicle is moving from one node to a different node.

In our formulation, we associate a binary variable to each state such that when they are equal to 1, it means that the EV is working as represented by the corresponding state. These variables are: $c_{bat,h,node}$, (for the state 'charging'), $i_{bat,h,node}$ (for the state 'injecting'), $o_{bat,h}$ (for the state 'disconnected') and $m_{bat,h}$ (for the state 'moving'). The subindexes are: $bat \in \Omega_{EV}$, h ∈ [0, 23] assuming a 24-hour planning horizon and *node* $\in \Omega_n$. To define the constraints imposed on these variables, we use the following equations:

$$\left(\sum_{\forall node \in \Omega_n} c_{bat,h,node} + i_{bat,h,node}\right) + d_{bat,h} \leq 1, \forall\, bat \in \Omega_{EV}, h \in [0,23] \quad (1)$$

$$\left(1 - d_{bat,h}\right) + m_{bat,h} \leq 1\,, \forall\, bat \in \Omega_{EV}, h \in [0,23] \quad (2)$$

Eq. 1 guarantees that the vehicle cannot exchange energy with the grid and be disconnected at the same time. Additionally, Eq. 2 requires that if an EV is moving it must also be disconnected.

Every state implies variations on the energy of the EV battery. Specifically, we define three real variables concerning the power changes along one time period (in terms of energy). These variables are $Pch_{bat,h,node}$, $Pin_{bat,h,node}$ y $Pmov_{bat,h} \in \mathbb{R}^+$; $\forall\, bat \in \Omega_{EV}, \forall\, node \in \Omega_n, \forall\, h \in [0,23]$ for the states 'charging', 'injecting' and 'moving' respectively. Additionally, we set three constants associated to the maximum power for each state. Thus, PC_{max} refers to the maximum power provided to charge the EV, PI_{max} corresponds to the maximum power the EV is allowed to inject to the grid and PM_{max} reflects the maximum power consumed by the EV when it is moving. The power-based variables and the constants are related as expressed by:

$$PC_{max} * c_{bat,h,node} \geq Pch_{bat,h,node}\,, \forall\, bat \in \Omega_{EV}, h \in [0,23], node \in \Omega_n \quad (3)$$

$$PI_{max} * i_{bat,h,node} \geq Pin_{bat,h,node}\,, \forall\, bat \in \Omega_{EV}, h \in [0,23], node \in \Omega_n \quad (4)$$

$$PM_{max} * m_{bat,h} \geq Pmov_{bat,h}\ , \forall\ bat\ \in\ \Omega_{EV}, h\ \in [0{,}23] \qquad (5)$$

Note that for simplicity, we assume one-hour time periods and hence, the conversion factor from kW to kWh is "1". Losses are considered for the charge and discharge processes by using parameters η_{ch} and η_{in}as the charge and injecting efficiencies respectively. Both values in the range [0,1]. Thus, the resulting energy delivered by the grid by an EV *bat* at a node during an hour *h* ($EVE_{bat,h,node}$) equals:

$$EVE_{bat,h,node} = \frac{Pch_{bat,h,node}}{\eta_{ch}} - Pin_{bat,h,node} * \eta_{in}, \quad \forall\ bat\ \in\ \Omega_{EV}, h\ \in [0{,}23], node\ \in \Omega_n \qquad (6)$$

The above defined power magnitudes need to be related to the amount of energy stored in the battery, which is represented by the SoC (State of charge) of the batteries. Thus, we know that $SOC_{bat,h}\ \in\ \mathbb{R}^+$ and that:

$$SOC_{bat,h}\ \leq SOC_{max};\ \forall\ bat\ \in\ \Omega_{EV}, h\ \in [0{,}23] \qquad (7)$$

$$SOC_{bat,h}\ \geq SOC_{min};\ \forall\ bat\ \in\ \Omega_{EV}, h\ \in [0{,}23] \qquad (8)$$

The value of this parameter varies according to the interaction the EV is performing with the grid and to the consumption it experiences if it is moving. Specifically, we define how the current value of SoC is related to the previous SoC as follows:

$$SOC_{bat,h+1} = SOC_{bat,h} * LB + \sum_{node\ \in \Omega_n}\left(Pch_{bat,h,node} - Pin_{bat,h,node}\right) - Pmov_{bat,h}\ , \quad \forall\ bat\ \in\ \Omega_{EV}, h\ \in [0{,}23] \qquad (9)$$

with

$$SOC_{bat,24} = SOC_{bat,0};\ \forall\ bat\ \in\ \Omega_{EV} \qquad (10)$$

As can be observed, even when there is neither exchange between the EV and the grid nor consumption due to movement, the SoC in the next interval decreases by a small amount fixed through parameter (LB) in Eq. 9. This decrement models the losses in a real battery due to leakages. This is a simplified model of the many mechanisms that take place during battery operation and which degrade the battery. However, we consider this model accurate enough for the purposes of the complete routing/scheduling algorithm. The proposed model also incorporates other consequences of the realistic performances of batteries. In particular, we restrict the maximum depth of discharge (DoD_{max}) and the total number of charge/discharge cycles that a battery withstands (NC_{max}). For the first restriction, we include the equation:

$$SOC_{bat,h}\ \geq SOC_{máx}\ * \frac{DoD_{max}}{100};\ \forall\ bat\ \in\ \Omega_{EV}, h\ \in [0{,}23] \qquad (11)$$

The second limitation is implemented by the following equation

$$\sum_{h=1,2,\dots}^{24} x_{bat,h} \leq 2 * (NC_{max}) - 1 \quad ,\forall\, bat \in \Omega_{EV} \tag{12}$$

where $x_{bat,h}$ is a binary variable in a matrix of dimensions $[size\,(\Omega_{EV}), 24]$. It represents whether there is a change in the behavior (charging, injecting) of the battery from its state in interval *h* to its state in interval *h+1*. If there is a change, its value equals 1, otherwise it is set to 0.

In order to correctly implement equation (12) above, we also use a new binary variable $w_{bat,h}$ of dimension $[size\,(\Omega_{EV}), 24]$. This variable indicates whether a vehicle is being charged at interval *h* (then its value is 1) or injecting power to the grid (its value is 0). When the vehicle is disconnected its value is also 1. Note that this variable differs from variable $c_{bat,h,node}$ in the fact that $w_{bat,h}$ does not contain information regarding the connection node.

The definition of variable $w_{bat,h}$ is formulated as follows:

$$w_{bat,h} \leq 1 - m_{bat,h} - \sum_{node\,\in\Omega_n} i_{bat,h,node} \quad ,\forall\, bat \in \Omega_{EV}, h \in [0,23] \tag{1}$$

$$w_{bat,h} \geq \sum_{node\,\in\Omega_n} c_{bat,h,node} \quad ,\forall\, bat \in \Omega_{EV}, h \in [0,23] \tag{2}$$

$$\left(w_{bat,h} - w_{bat,h+1}\right) \geq x_{bat,h} \quad ,\forall\, bat \in \Omega_{EV}, h \in [0,23] \tag{3}$$

$$\left(w_{bat,h+1} - w_{bat,h}\right) \geq x_{bat,h} \quad ,\forall\, bat \in ?\ \Omega_{EV}, h \in [0,23] \tag{4}$$

Note that without the use of variable $w_{bat,h}$ equations (15) and (16) would be more complicated, as they would have to include summations over all the nodes of the $c_{bat,h,node}$ variables; thus the intermediate use of the $w_{bat,h}$ variables allows for faster problem solving.

Spatial behavior

Due to its movement, the vehicle changes its connection to the electrical network. To represent these modifications, we rely on the following binary variables:

- $e_{bat,h,node}$. It is a 3-dimensional data structure with dimensions $[size(\Omega_{EV}), 24, size(\Omega_N)]$. When its value is 1, it means that the EV bat is connected to node *node* during interval *h*. If this condition does not hold,

the value of the variable equals 0. As the EV can only be connected to one node, we impose:

$$\sum_{node \in \Omega_n} e_{bat,h,node} = 1 \quad , \forall\ bat\ \in\ \Omega_{EV}, h\ \in [0,23] \tag{17}$$

- $d_{bat,h,node\_o,node\_d}$. It is included in a 4-dimensional binary data structure with dimensions $[size(\Omega_{EV}), 24, size(\Omega_N), size(\Omega_N)]$. When its value is 1, it represents that the EV *bat* is moving from *node_o* to *node_d* at time interval *h*. The movement can only happen between two particular nodes and this restriction is modeled with the following equation:

$$\sum_{node_o \in \Omega_n} \sum_{node_d \in \Omega_n} d_{bat,h,node_o,node_d} \leq 1 \quad , \quad \forall\ bat\ \in\ \Omega_{EV}, h\ \in [0,23] \tag{18}$$

An interval *h* is sufficient to complete any movement so the following equations impose that the EV must be at the origin of any movement when the transition begins and must be at the destination when the movement ends:

$$e_{bat,h,node_o} \geq d_{bat,h,node_o,node_d} \quad , \forall\ bat\ \in\ \Omega_{EV}, \quad h\ \in [0,23], node\_o, node\_d \in \Omega_n \tag{19}$$

$$e_{bat,h+1,node_d} \geq d_{bat,h,node_o,node_d} \quad , \forall\ bat\ \in\ \Omega_{EV}, \quad h\ \in [0,23], node\_o, node\_d \in \Omega_n \tag{20}$$

Both variables are related with a new binary variable named $a_{bat,h,node}$ as expressed in the following equations:

$$a_{bat,h,node} \geq e_{bat,h,node} + e_{bat,h+1,node} - 1\ , \quad \forall\ bat\ \in\ \Omega_{EV}, h\ \in [0,23], node\ \in \Omega_n \tag{21}$$

$$1 - m_{bat,h} = \sum_{node \in \Omega_n} a_{bat,h,node} \quad , \qquad \forall\ bat\ \in\ \Omega_{EV}, h\ \in [0,23] \tag{22}$$

This means that the movement variable is consistent with the fact that the EV cannot move if its location variables indicate that its location is not changed for one period of time.

The charging and discharging operations restrict the EV mobility so that the vehicle needs to be static and connected to the grid for both procedures. These requirements are expressed with the following equations:

$$c_{bat,h,node} \leq e_{bat,h,node} \quad ,\forall\ bat\ \in\ \Omega_{EV}, h\ \in [0,23], node\ \in \Omega_n \tag{23}$$

$$i_{bat,h,node} \leq e_{bat,h,node} \quad ,\forall\ bat\ \in\ \Omega_{EV}, h\ \in [0,23], node\ \in \Omega_n \tag{24}$$

The movement of the vehicle implies changes in the power stored in its battery. We assume that the types of roads are uniform for the area studied so that the consumption only depends on the physical distance from *node_o* to *node_d*. In particular, we manage the matrix *DistN*, with dimensions [(*size* Ω_n), (*size* Ω_n)]. This data structure keeps the information related to the physical distance between the nodes. Consequently,

$$\sum_{node_o \in \Omega_n} \sum_{node_d \in \Omega_n} DistN_{node_o,node_d} * d_{bat,h,node_o,node_d} * Pcons_B = Pcar_{bat,h}, \quad \forall\ bat\ \in\ \Omega_{EV}, h\ \in [0,23] \tag{25}$$

Finally, we also restrict the maximum number of chargers (NC) connected to any node. Thus:

$$\sum_{bat \in \Omega_{EV}} c_{bat,h,node} + i_{bat,h,node}\ \leq\ NC\ ,\forall\ node\ \in \Omega_n, h\ \in [0,23] \tag{26}$$

3. Joint routing and scheduling algorithms for bidirectional power transfer

As mentioned previously, routing and scheduling could be used for diverse purposes and could be solved independently, sequentially or jointly. Figure 1 shows how the sequential procedure first solves the routing problem based on the EVs position constraints (their origins and their destinations), and then the scheduling algorithm is employed with the computed routes, the network status and the market prices to determine the recommended scheduling for the charge and the discharge processes.

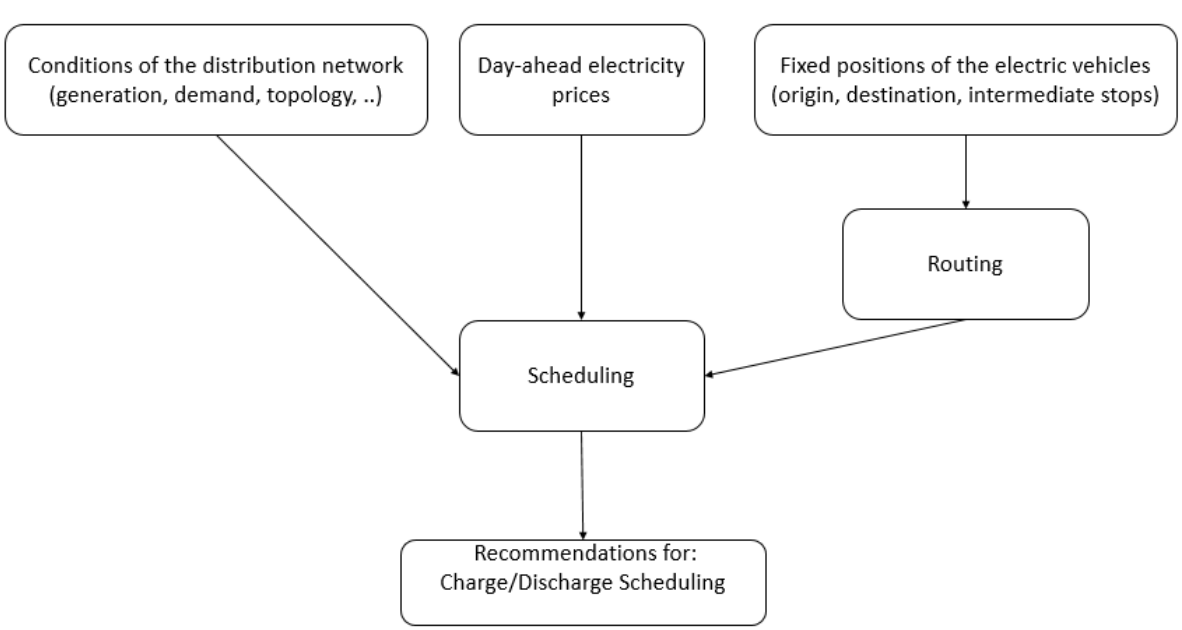

Figure 1. Scheme of the sequential routing and scheduling algorithm.

In this paper we define a joint routing and scheduling algorithm. The flowchart is illustrated in Figure 2. Based on spatial EV constraints, the network features and the day-ahead market prices, the developed model is able to simultaneously solve how the routing and scheduling should be performed in order to maximize users' profits.

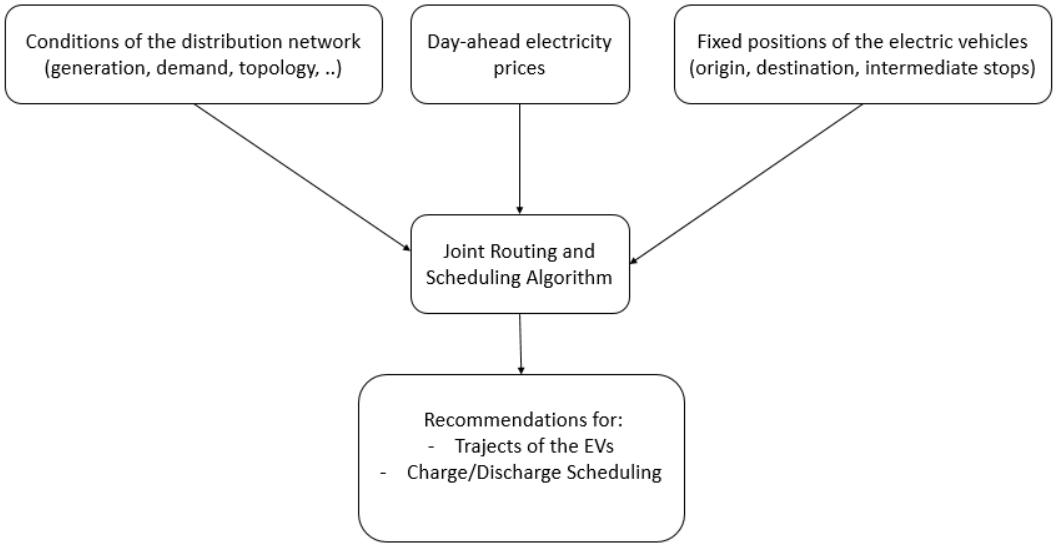

Figure 2. Scheme for the joint routing and scheduling algorithm.

The algorithm is based on an optimization problem that is built on the EVs models (as explained in Section 2), the network performance and the drivers' interactions. These latter two issues are explained next.

3.1 Model of network performance

Eqs. 27-29 model the constraint regarding the real operation of generators; these generators may be turned off and on as needed. First, Eq. 27 restricts the maximum power delivered by the generator. The change in power output is limited by the ramping-up and down (*Rup* and *Rdown* respectively). These parameters depend on the generator type so we include the subindex *gen* to indicate generator type.

$$P_{gen,node,h+1} \geq P_{gen,node,h} - Rdown_{gen}\,, \forall\ node\ \in \Omega_n, h\ \in [0,23] \tag{27}$$

$$P_{gen,node,h+1} \leq P_{gen,node,h} + Rup_{gen}\,, \forall\ node\ \in \Omega_n, h\ \in [0,23] \tag{28}$$

The following equations model the network power balance. Specifically, Eq. 29 reflects the power balance at the nodes where EVE was defined in the EV electrical model. EVE represents the energy exchange between the electric vehicles and the grid. Eq. 30 is the injection equation for a given node. A DC model approximation is used. The maximum power flow is restricted by Eq. 31. Concerning the demand included in Eq. 30, we assume a time-varying demand.

$$P_{gen,node,h} + flow_{node,h} = Demand_{node,h} + \sum_{bat\,\in\Omega_{EV}} EVE_{bat,h,node}\ \ , \quad \forall\ node\ \in \Omega_n, h\ \in [0,23] \tag{29}$$

$$flow_{node\_i,h} = \sum_{node\_j\,\in\Omega_n}^{node\_i} \Big(SL_{node\_i,node\_j} * \left(\emptyset_{node_i,h} - \emptyset_{node_j,h}\right) + SL_{node\_j,node\_i} * \left(\emptyset_{node\_i,h} - \emptyset_{node\_j,h}\right)\Big) \tag{30}$$

$$SL_{node_i,node_j} * \left(\emptyset_{node_i,h} - \emptyset_{node_j,h}\right) \leq MaxFlow_{node_i,node_j}\,, \quad \forall\ node\_i, node\_j\ \in \Omega_n, h\ \in [0,23] \tag{31}$$

3.2 Maximizing the users' benefits

The proposed joint routing and scheduling algorithm aims at maximizing the users' revenues ($benefit_{day}$) obtained from the energy that they deliver to the grid. This strategy could stimulate user participation in the grid market.

The formulation of the problem to solve is as follows:

$$MAX: benefit_{day} \tag{32}$$

subject to:

$$benefit_{day} = \sum_{h=0}^{23} benefit_h \tag{33}$$

$$benefit_h = \sum_{bat \in \Omega_{EV}} \sum_{node \in \Omega_n} Pin_{bat,h,node} * p\_o_{h,node} - \sum_{bat \in \Omega_{EV}} \sum_{node \in \Omega_n} Pch_{bat,h,node} * \quad p\_d_{h,node}, \forall h \in [0,23] \tag{34}$$

with *p_o being* the price offered by the electrical system to buy energy at a specific node and time and *p_d being* the price offered by the electrical system to users to sell their energy at a particular node and time. For our problem, both magnitudes are considered input data.

It can be observed that a user's profit corresponds to the difference between the profit generated by the energy delivery that she produces and the costs associated with the charge of her vehicle.

4. Analysis of the simulation results

The performance of the proposed mathematical framework is verified by means of simulations. The GAMS framework (General Algebraic Modeling System), which is oriented to optimization problems, is used for this purpose. In particular, the MIP (mixed integer programming) solver is used due to the mathematical features of the proposed formulation. According to the formulation proposed in this paper, the joint scheduling and routing algorithm is a mixed-integer linear programming.

4.1 Scenario under evaluation

The network under study is based on the modified IEEE 37-node test feeder, which is used for testing technologies associated with distribution networks [22]. This network comprises 37 nodes and 37 lines. A representation of the network with vehicle chargers and generators is in Figure 3. Generators are identified with the term *G* (ranging from G1 to G11). It can be observed that the maximum number of chargers per node is 3.

Regarding the demands, these are summarized in Table I in the Appendix.

In order to model a realistic behavior of the demand, this parameter is not constant but varies during the day. Thus, demand for a specific hour of the day is computed as the values shown in Table I multiplied by the corresponding hour-dependent coefficient presented in Table II. Table II is also included in the Appendix.

On the other hand, the susceptance and the maximum power flow associated with the lines are presented in Table III in the Appendix.

Regarding generation units, there are 11 of these divided into three types as in [18]. For each type, the parameters concerning their generation are in Table IV.

Table IV. Characteristics of the generation units.

Type	$P_{max,gen}$ (MW)	Rup (kW)	$Rdown$ (kW)
1	100	50	50
2	200	150	150
3	250	50	50

The generation identification, their type and the node to which they are connected are presented in Table IV. Table IV is in the Appendix.

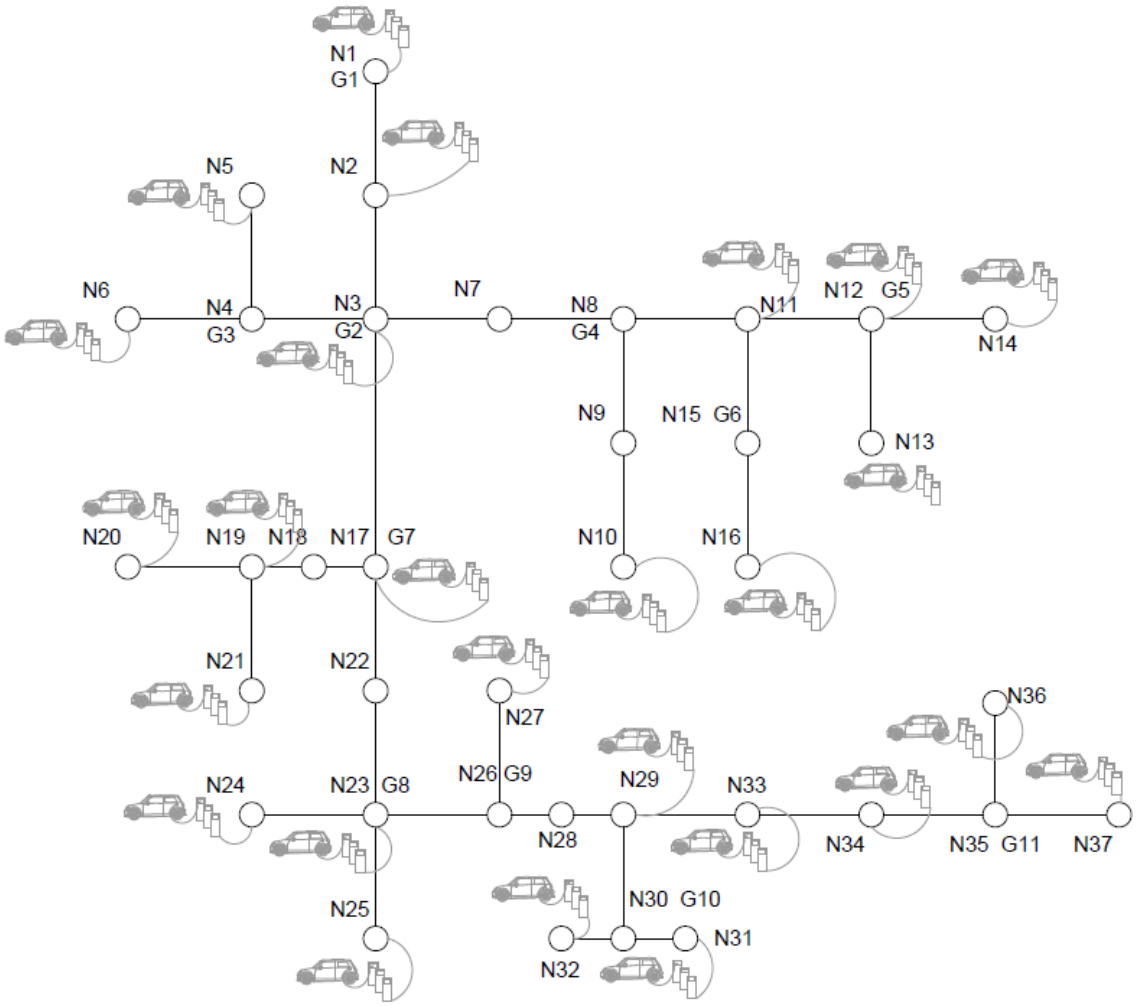

Figure 3. Illustration of the network under test where the generators and chargers are also shown.

In our scenario, there are 12 EVs, which can be grouped into three classes according to their behavior: class-A (5 EVs), class-B (5 EVs) and class-C (2 EVs). For all the vehicles, we assume that the initial (at hour 0) and the final (at hour 23) SOC equal 5%. Class-A vehicles belong to owners living in node 11. It takes them 2 hours to drive to their office, which is located in node 28. Class-B vehicles also model the driving patterns of

users going to their workplace every day. In particular, they reside in the area around node 25 and their work destinations are in node 33. The commute takes 1 hour. During working hours, the vehicles are assumed to have no connection to the grid as not all the work places will necessarily be fitted with charging equipment. Finally, Class-C vehicles are delivery trucks, which cross the city during working hours. They visit multiple nodes in the network. Specifically, one Class-C vehicle starts at 8am in node 19 and visits nodes 4, 2, 9 and 15. At hour 17, it has to leave the car in a deposit attached to node 12. There is another Class-C truck, which starts at node 12 and is required to visit node 35 and 32. This car must be left at hour 17 at node 12. The visiting nodes of Class-C vehicles have been selected in order to define a delivery system that crosses the entire network with its trucks.

The vehicles are equipped with batteries; these batteries are described in Table VI.

Table VI. Battery features.

$\boldsymbol{\eta_{car}}$	$\boldsymbol{\eta_{in}}$	$\boldsymbol{PC_{max}}$	$\boldsymbol{PI_{max}}$	$\boldsymbol{PM_{max}}$
95%	99%	3.7 kW	3.7 kW	4.8 kWh
$\boldsymbol{SOC_{max}}$	$\boldsymbol{DoD_{max}}$	$\boldsymbol{NC_{max}}$	$\boldsymbol{PBcons}$	$\boldsymbol{LB}$
16.5 kWh	80%	4	0.12 kW/Km	99%

Regarding the electricity market, the prices for the energy bought and sold in the V2G operations (*p_d* and *p_o* variables in the mathematical model), have been set in a realistic manner, based on node demand. In particular, we have defined a base price equal to 11.54 cent/kWh for the buying operations (the vehicle is charged) and a base price of 18.64 cent/kWh for the selling operations (the vehicle is actively discharged).

The sale and buy prices are not constant. Firstly, the reference price for the sale in each node depends on its demand. Taking into account the demand, we define the following reference prices for the energy sold by the vehicles in Table VII. Table VII is included in the Appendix. According to these values, nodes 2, 6, 13, 20, 33 and 34 offer higher revenues for the drivers in the energy sale process when connected to them.

In addition, both the sale and the buy prices depend on the time at which the V2G operation occurs. Thus, the reference prices defined previously are multiplied by the coefficients in Table VIII according to the time of the energy transfer. Table VIII is contained in the Appendix. It is noted that, during the night, the system favors vehicle charging as the purchase prices are lower. In contrast, during the day, the purchase prices are higher than the sale prices.

4.2 Results and analysis:

This study makes an analysis of the suitability of applying a joint routing and scheduling algorithm that may recommend that drivers make some small changes to their expected journeys in order to perform a charge/discharge process. Table IX compares the results obtained when the joint algorithm is applied to the results derived from the sequential application of the routing and the scheduling algorithms.

The combination of routing and scheduling in one optimization model leads to longer journeys for class-A and class-B drivers (25% and 5% longer respectively). These longer routes allow for a significant increase in the energy trading performed by the vehicles. It can be observed that class-B drivers would experience 50% more energy transfer when the joint model is applied in comparison with the sequential execution of routing and scheduling, and this is achieved with only 5% longer routes. The increase in the energy transfer of class-A drivers is nearly 20% with the joint routing and scheduling algorithm. As an initial conclusion, we can state that there is not a proportional relationship between the increment in the length of the route and the increase of the energy transfer; however, we can conclude that the joint application of the routing and scheduling algorithm favors the V2G operations.

We also observe that the recommendations for deviations in the routes take journey restrictions into consideration. This behavior is evident in class-C vehicles where the joint algorithm does not result in routes that are longer than the shortest routes resulting from the sequential routing and scheduling algorithm.

Concerning losses, these are proportional to the energy transfer in the two algorithms evaluated as it models a realistic behavior of the electrical network.

Table IX. Results of running the joint and the routing/scheduling sequential algorithm

		Joint Routing and Scheduling algorithm	Sequential Routing and Scheduling algorithm
Class-A vehicles	Energy charged (kWh)	163.59	135.35
	Energy injected (kWh)	79.11	66.84
	Distance traveled by the group (km)	595	475
	Losses in the charge process (kWh)	8.18	6.76
	Losses in the injection process (kWh)	0.79	0.66
Class-B vehicles	Energy charged (kWh)	148.48	98.53
	Energy injected (kWh)	84.86	38.6
	Distance traveled (km)	420	400
	Losses in the charge process (kWh)	7.4	4.92
	Losses in the injection process (kWh)	0.84	0.39
Class-C vehicles	Energy charged (kWh)	49.06	48.93
	Energy injected (kWh)	8.62	8.6
	Distance traveled (km)	300	300
	Losses in the charge process (kWh)	2.45	2.4
	Losses in the injection process (kWh)	0.08	0.08

If we pay attention to the revenues that the users obtain, the differences are clear. When following the joint strategy, the drivers obtain a total of 1661.94 cents in one day. This parameter is much greater than the benefits reported by the sequential

application of routing and scheduling. In this approach, the total revenues are 265.40 cents in one day. It can be concluded that minor changes to drivers' journeys result in significant increase in their profits.

Consequently, the algorithm for the joint decision regarding the EV routes and their schedules for the V2G operations clearly increases the energy transfer processes if it is feasible to alter the vehicles' route. As a result, the drivers gain significant revenues. With these benefits in mind, it is recommended that some fleets of vehicles (e.g. delivery trucks) should be managed according to the proposed joint algorithm.

5. Conclusions

This paper has focused on the operation of an EV fleet with V2G capabilities where EVs users decide when and where they exchange energy with the grid. In particular, a mixed-integer linear programming formulation has been presented to jointly perform the routing of the electric vehicles and the scheduling of their charge/discharge operation. By combining both processes, the EV drivers are recommended to make minor changes to the classical routing and charging pattern behavior in order to increase their revenues. The results show that slight deviations from conventional user behavior (related to their movements and charging/discharging pattern) lead to significant increases in energy transfer. This generates significant revenue, which encourages driver participation in this electricity market. The algorithm takes into account the restrictions regarding the positions that the EV drivers may impose. Due to this advantage and the fact that drivers are recommended to make small deviations (5% in one of the cases evaluated in the paper), the application of the joint algorithm is of interest.

Acknowledgments:

This work has been partially funded by the project ENE2016-80638-R granted by Ministerio de Economía y Competitividad of the Government of Spain.

APPENDIX

This section includes some data related to the scenario evaluated.

Table I. Demand on each node for the IEEE-37 electrical network under study.

Node	Demand (kW)	**Node**	Demand (kW)	**Node**	Demand (kW)
N1	0	**N14**	42	**N27**	42
N2	100	**N15**	0	**N28**	85
N3	0	**N16**	42	**N29**	42
N4	0	**N17**	0	**N30**	0
N5	85	**N18**	42	**N31**	42

N6	93	**N19**	42	**N32**	85
N7	85	**N20**	126	**N33**	140
N8	0	**N21**	42	**N34**	126
N9	38	**N22**	85	**N35**	0
N10	85	**N23**	0	**N36**	85
N11	85	**N24**	85	**N37**	42
N12	0	**N25**	0		
N13	161	**N26**	0		

Table II. Hourly multiplying coefficient for the demand

Hour	**1**	**2**	**3**	**4**	**5**	**6**	**7**	**8**	**9**	**10**	**11**	**12**
Coeffficient	0,6	0,5	0,4	0,35	0,4	0,5	0,6	0,7	0,8	0,9	0,95	0,95
Hour	**13**	**14**	**15**	**16**	**17**	**18**	**19**	**20**	**21**	**22**	**23**	**24**
Coefficient	1.1	1	0,9	0,8	0,7	0,8	0,9	0,95	1.1	0,95	0,8	0,7

Table III. Susceptance and maximum power flow for each line in the IEEE-37 electrical network under study.

Line	**Susceptance (siemens)**	**Maximum Power Flow (MW)**	**Line**	**Susceptance (siemens)**	**Maximum Power Flow (MW)**
N1.N38	117.6471	4.6973	**N17.N22**	426.1650	1.5796
N38.N2	578.7299	4.6973	**N18.N19**	913.2107	1.5796
N2.N3	799.8738	3.3255	**N19.N20**	446.4397	1.0808
N3.N4	223.2198	1.0808	**N19.N21**	318.8855	1.0808
N3.N7	710.2750	1.5796	**N22.N23**	1278.4950	1.5796
N3.N17	581.7264	3.3255	**N23.N24**	426.1650	1.5796
N4.N5	372.0330	1.0808	**N23.N25**	110.2247	1.0808
N4.N6	279.0248	1.0808	**N23.N26**	799.0594	1.5796
N7.N8	491.7289	1.5796	**N26.N27**	279.0248	1.0808
N8.N9	1116.0991	1.0808	**N26.N28**	799.0594	1.5796
N8.N11	319.6238	1.5796	**N28.N29**	456.6054	1.5796
N9.N10	171.7076	1.0808	**N29.N30**	171.7076	1.0808
N11.N12	97.0521	1.0808	**N29.N33**	399.5297	1.5796
N11.N15	426.1650	1.5796	**N30.N31**	69.7562	1.0808
N12.N13	744.0661	1.0808	**N30.N32**	446.4397	1.0808
N12.N14	117.4841	1.0808	**N33.N34**	639.2475	1.5796
N15.N16	318.8855	1.0808	**N34.N35**	639.2475	1.5796
N17.N18	372.0330	1.0808	**N35.N36**	446.4397	1.0808
			N35.N37	639.2475	1.5796

Table V. Generator connection and type.

Generator Identification	Type	Node	Generator Identification	Type	Node
G1	1	N1	G7	3	N17
G2	1	N3	G8	2	N23
G3	2	N4	G9	3	N26
G4	2	N8	G10	2	N30
G5	3	N12	G11	3	N35
G6	1	N15			

Table VII. Reference price for the sale operation in each electrical node.

Node	**Reference Price for the sale operation (cent/kWh)**	**Node**	**Reference Price for the sale operation (cent/kWh)**	**Node**	**Reference Price for the sale operation (cent/kWh)**
N1	0	N14	9.69	N26	0
N2	23.08	N15	0	N27	9.69
N3	0	N16	9.69	N28	19.62
N4	0	N17	0	N29	9.69
N5	19.62	N18	9.69	N30	0
N6	21.46	N19	9.69	N31	9.69
N7	19.662	N20	29.08	N32	9.69
N8	0	N21	9.69	N33	32.31
N9	8.7704	N22	19.62	N34	29.08
N10	19.62	N23	0	N35	0
N11	19.62	N24	19.62	N36	19.62
N12	0	N25	0	N37	9.81
N13	37.16				

Table VIII. Multiplying coefficient for the purchase and sale reference prices in the V2G operations.

Hour	**Coefficient for buying energy**	**Coefficient for selling energy**	**Hour**	**Coefficient for buying energy**	**Coefficient for selling energy**
Hour 1	0.5	0.6	Hour 13	1.1	1.05
Hour 2	0.4	0.5	Hour 14	1	1
Hour 3	0.3	0.4	Hour 15	0.95	0.95
Hour 4	0.35	0.45	Hour 16	0.95	0.9
Hour 5	0.4	0.5	Hour 17	0.9	0.8
Hour 6	0.45	0.6	Hour 18	1	0.95
Hour 7	0.6	0.7	Hour 19	1.1	1
Hour 8	0.8	0.8	Hour 20	1.1	1.05
Hour 9	0.9	0.9	Hour 21	1.05	1

Hour 10	1	0.95	Hour 22	0.95	0.95
Hour 11	1.1	1.05	Hour 23	0.75	0.8
Hour 12	1.2	1.1	Hour 24	0.65	0.7

References

[1] N. Shaukat, B. Khan, S. M. Ali, C. A. Mehmood, J. Khan, U. Farid, M. Majid, S. M. Anwar, M. Jawad, and Z. Ullah, "A survey on electric vehicle transportation within smart grid system," *Renew. Sustain. Energy Rev.*, Jun. 2017.

[2] G. Razeghi and S. Samuelsen, "Impacts of plug-in electric vehicles in a balancing area," *Appl. Energy*, vol. 183, pp. 1142–1156, Dec. 2016.

[3] K. M. Tan, V. K. Ramachandaramurthy, and J. Y. Yong, "Integration of electric vehicles in smart grid: A review on vehicle to grid technologies and optimization techniques," *Renew. Sustain. Energy Rev.*, vol. 53, pp. 720–732, Jan. 2016.

[4] J. Hu, H. Morais, T. Sousa, and M. Lind, "Electric vehicle fleet management in smart grids: A review of services, optimization and control aspects," *Renew. Sustain. Energy Rev.*, vol. 56, pp. 1207–1226, Apr. 2016.

[5] C. Peng, J. Zou, L. Lian, and L. Li, "An optimal dispatching strategy for V2G aggregator participating in supplementary frequency regulation considering EV driving demand and aggregator's benefits," *Appl. Energy*, vol. 190, pp. 591–599, Mar. 2017.

[6] E. Demir, T. Bektaş, and G. Laporte, "The bi-objective Pollution-Routing Problem," *Eur. J. Oper. Res.*, vol. 232, no. 3, pp. 464–478, Feb. 2014.

[7] A. Franceschetti, D. Honhon, T. Van Woensel, T. Bektaş, and G. Laporte, "The time-dependent pollution-routing problem," *Transp. Res. Part B Methodol.*, vol. 56, pp. 265–293, Oct. 2013.

[8] A. D. Jovanović, D. S. Pamučar, and S. Pejčić-Tarle, "Green vehicle routing in urban zones – A neuro-fuzzy approach," *Expert Syst. Appl.*, vol. 41, no. 7, pp. 3189–3203, Jun. 2014.

[9] C. G. Hoehne and M. V. Chester, "Optimizing plug-in electric vehicle and vehicle-to-grid charge scheduling to minimize carbon emissions," *Energy*, vol. 115, pp. 646–657, Nov. 2016.

[10] S. Tabatabaee, S. S. Mortazavi, and T. Niknam, "Stochastic scheduling of local distribution systems considering high penetration of plug-in electric vehicles and renewable energy sources," *Energy*, vol. 121, pp. 480–490, Feb. 2017.

[11] A. Janjic, L. Velimirovic, M. Stankovic, and A. Petrusic, "Commercial electric vehicle fleet scheduling for secondary frequency control," *Electr. Power Syst. Res.*, vol. 147, pp. 31–41, Jun. 2017.

[12] K. Knezović, A. Soroudi, A. Keane, and M. Marinelli, "Robust multi-objective PQ scheduling for electric vehicles in flexible unbalanced distribution grids," *IET Gener. Transm. Distrib.*, vol. 11, no. 16, pp. 4031–4040, Nov. 2017.

[13] D. C. Paraskevopoulos, G. Laporte, P. P. Repoussis, and C. D. Tarantilis, "Resource constrained routing and scheduling: Review and research prospects," *Eur. J. Oper. Res.*, May 2017.

[14] B. Yagcitekin and M. Uzunoglu, “A double-layer smart charging strategy of electric vehicles taking routing and charge scheduling into account,” *Appl. Energy*, vol. 167, pp. 407–419, Apr. 2016.

[15] J. Barco, A. Guerra, L. Muñoz, and N. Quijano, “Optimal Routing and Scheduling of Charge for Electric Vehicles: A Case Study,” *Math. Probl. Eng.*, vol. 2017, pp. 1–16, Nov. 2017.

[16] T. Chen, B. Zhang, H. Pourbabak, A. Kavousi-Fard, and W. Su, “Optimal Routing and Charging of an Electric Vehicle Fleet for High-Efficiency Dynamic Transit Systems,” *IEEE Trans. Smart Grid*, pp. 1–1, 2016.

[17] H. Yang, Y. Deng, J. QIU, M. Li, M. Lai, and Z. Y. Dong, “Electric Vehicle Route Selection and Charging Navigation Strategy based on Crowd Sensing,” *IEEE Trans. Ind. Informatics*, pp. 1–1, 2017.

[18] H. Yang, S. Yang, Y. Xu, E. Cao, M. Lai, and Z. Dong, “Electric Vehicle Route Optimization Considering Time-of-Use Electricity Price by Learnable Partheno-Genetic Algorithm,” *IEEE Trans. Smart Grid*, vol. 6, no. 2, pp. 657–666, Mar. 2015.

[19] J. Tan and L. Wang, “Real-Time Charging Navigation of Electric Vehicles to Fast Charging Stations: A Hierarchical Game Approach,” *IEEE Trans. Smart Grid*, pp. 1–1, 2015.

[20] A. Abdulaal, M. H. Cintuglu, S. Asfour, and O. A. Mohammed, “Solving the Multivariant EV Routing Problem Incorporating V2G and G2V Options,” *IEEE Trans. Transp. Electrif.*, vol. 3, no. 1, pp. 238–248, Mar. 2017.

[21] W. Tang, S. Bi, Y. J. Zhang, and X. Yuan, “Joint Routing and Charging Scheduling Optimizations for Smart-Grid Enabled Electric Vehicle Networks,” in *2017 IEEE 85th Vehicular Technology Conference (VTC Spring)*, 2017, pp. 1–5.

[22] IEEE 37-Bus Feeder, IEEE PES Distribution System Analysis Subcommittee's Distribution Test Feeder Working Group, [Online]. Available: http://ewh.ieee.org/soc/pes/dsacom/testfeeders/index.html